DOI: 10.1002/ejic.200700287

Synthesis, Characterization, and Sensitizing Properties of Heteroleptic Ru^{II} Complexes Based on 2,6-Bis(1-pyrazolyl)pyridine and 2,2′-Bipyridine-4,4′-dicarboxylic Acid Ligands

Athanassios I. Philippopoulos,*[a][‡] Aris Terzis,[b] Catherine P. Raptopoulou,[b] Vincent J. Catalano,[c] and Polycarpos Falaras*[a]

Keywords: 2,6-Bis(1-pyrazolyl)pyridine / Heteroleptic Ru^{II} complexes / Dye-sensitized solar cells / Ruthenium / Protonation

Starting from the $Ru(bpp)Cl_3$ precursor (**1**), a family of novel heteroleptic Ru^{II} complexes of the general formulae [Ru(bpp)(dcbpyH)(X)] [X = Cl^- (**2a**), NCS^-, (**3**)] and Na[Ru(bpp)(dcbpy)(CN)] (**4**) with the ligands 2,6-bis(1-pyrazolyl)pyridine (bpp) and 2,2′-bipyridine-4,4′-dicarboxylic acid ($dcbpyH_2$) has been synthesized, spectroscopically characterized, and attached to nanocrystalline TiO_2 electrodes to be tested as solar cell sensitizers. Addition of HCl to (**2a**) led to the corresponding cationic derivative $[Ru(bpp)(dcbpyH_2)Cl]Cl$ (**2b**). All complexes were characterized by FT-IR, FT-Raman, UV/Vis, ^1H NMR spectroscopy, elemental analysis, and mass spectrometry. Complex **4** and the previously reported $[Ru(bdmpp)(dcbpyH_2)Cl](PF_6)$ (**5**) [bdmpp is 2,6-bis(3,5-dimethyl-1-pyrazolyl)pyridine] were characterized by single-crystal X-ray diffraction. The photo-electochemical properties of the dyes **2**–**4** were investigated and the efficiency of the corresponding dye-sensitized solar cells was compared to the sensitizing performance of the *cis*-$[Ru(dcbpyH)_2(NCS)_2](NBu_4)_2$ (**N719**) dye.

Introduction

During the last decade, nanocrystalline titania films sensitized by transition-metal complexes have been extensively used for the conversion of light to electricity, because of their high efficiency (approximately 10%) and low cost.[1] The so-called dye-sensitized solar cells (DSSCs) consist of a photoanode, a sensitizer chemically adsorbed on the surface of a mesoporous oxide layer, and a counter electrode sandwiching an electrolyte containing the redox couple (usually the I^-/I_3^- system in an organic medium).[2] Undoubtedly one of the most important parts of the cell is the sensitizer, mainly a ruthenium(II) polypyridine complex bearing suitable anchoring groups (carboxylic or phosphonic) for efficient grafting to the oxide surface via ester-type bond formation.[3] These dyes have to fulfill many other requirements like intense absorption in the visible region, efficient electron injection to the conduction band of the semiconductor, high stability of the sensitizer molecule, and reversibility of its redox chemistry.[4] Also, the electron transfer from the excited state of the dye to the semiconductor (TiO_2) should be very fast in comparison with decay to the ground state of the dye. Broad spectral response covering the entire visible range extending to the near-IR region is one of the most important prerequisites of a potential molecular sensitizer.

There is now a significant scientific effort for the development of efficient sensitizers with improved spectroscopic-photovoltaic characteristics for solar cell applications. Thus, a series of homoleptic $[Ru(L)_3]^{2+}$ and heteroleptic $[Ru(L^1)(L^2)(L^3)]^{2+}$, $[Ru(L^1)(L^2)(NCS)_2]$ (L = substituted bipyridyl with appropriate anchoring groups) ruthenium(II) complexes have been prepared.[5,6] So far one of the best sensitizers is *cis*-$[Ru(dcbpyH_2)_2(NCS)_2]$, known as N3, with a solar to electricity efficiency as high as 11.04%.[7] Moreover, a cell with extra pure monoprotonated *cis*-$[Ru(dcbpyH)_2(NCS)_2](NBu_4)_2$ (**N719** sensitizer), equipped with an antireflecting coating, gave an overall conversion efficiency of 11.18%. Use of modified ligands endowed with hydrophobic groups[8] and supramolecular functionalities has been proved to facilitate dye/redox couple interaction and dye regeneration.[9] On the basis of a judicious substitution of the bidentate by a tridentate ligand, a tris(isothiocyanato)-(4,4′,4′′-tricarboxy-2,2′:6,2′′-terpyridine)ruthenium(II) complex, so called black dye,[10] with a conversion efficiency of 10.4%, was proved to exhibit similar photovoltaic properties to the N3 dye. To further explore this possibility, 2,6-bis(3,5-dimethyl-1-pyrazolyl)pyridine

[a] NSCR "Demokritos", Institute of Physical Chemistry, Aghia Paraskevi Attikis, 15310 Greece
Fax: +30-210-6511766
E-mail: papi@chem.demokritos.gr
[b] NSCR "Demokritos", Institute of Material Science, Aghia Paraskevi Attikis, 15310 Greece
[c] Department of Chemistry, University of Nevada, Reno, NV 89557, USA
[‡] Current address: Inorganic Chemistry Laboratory, Department of Chemistry, National and Kapodistrian University of Athens, Panepistimiopolis, Zografou 15771, Greece
Fax: +30-210-7274782
E-mail: atphilip@chem.uoa.gr

(bdmpp)[11] (Scheme 1), a tridentate analogue to the terpyridine ligand, has been introduced in a Ru^{II} metal center.[12]

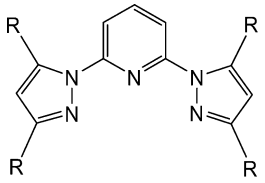

bpp: R = H; bdmpp: R = Me

Scheme 1. Structural formula of the ligands bpp and bdmpp.

In this respect, in our laboratory, we set out to synthesize ruthenium(II) molecular sensitizers using both the bdmpp and $dcbpyH_2$ ligands. Such a synthesis allows us to study the properties of the complexes and evaluate their influence on the performance of the corresponding dye-sensitized solar cells. As a result, the heteroleptic complexes $[Ru(bdmpp)(dcbpyH_2)(X)](PF_6)$ have been synthesized and successfully examined for the sensitization process.[13] In a more systematic approach towards this aim, i.e. the preparation of alternatives for the N3 and the corresponding black dye, in this paper, we report the synthesis and spectroscopic characterization of a series of neutral [Ru(bpp)(dcbpyH)(X)] (X = Cl^-, NCS^-) (**2a**, **3**), cationic $[Ru(bpp)(dcbpyH_2)Cl]Cl$ (**2b**), and anionic Na[Ru(bpp)-(dcbpy)(CN)] (**4**) ruthenium(II) complexes containing the tridentate ligand 2,6-bis(1-pyrazolyl)pyridine. Furthermore, their photo-electrochemical properties have been studied in sandwich-type solid-state nanocrystalline TiO_2 cells using a composite polymer redox electrolyte, namely PEO/TiO_2/I^-/I_3^-,[14] (PEO = polyethylene oxide, MW = 2×10^6) and compared to those of the corresponding $[Ru(bdmpp)(dcbpyH_2)-(X)](PF_6)$.[13]

Results and Discussion

Syntheses

The complexes **1**–**4** were synthesized by a route analogous to that reported previously.[13] The synthetic procedure for the preparation of complexes **1**–**2a** is shown in Scheme 2. Reaction of the precursor $Ru(bpp)Cl_3$ (**1**)[15] with the 2,2′-bipyridine-4,4′-dicarboxylic acid ligand in refluxing ethanol/water (1:1, v/v) and in the presence of Et_3N (acting as both reducing and deprotonating agent) afforded selectively the heteroleptic neutral complex [Ru(bpp)(dcbpyH)-Cl] (**2a**), which was isolated as a red-brown microcrystalline solid in 97% yield. It is a stable solid that does not decompose after heating at 215 °C. Its structure is similar to that reported for the [Ru(bmipy)(dcbpyH)I] [bmipy = 2,6-bis(1-methylbenzimidazol-2-yl)pyridine compound,[16] taking into consideration, that both octahedral complexes bear a tridentate (coordinated via nitrogen atoms), a halide, and a deprotonated (dcbpyH) 2,2′-bipyridine-4,4′-dicarboxylic acid] ligands around the Ru^{II} metal center.

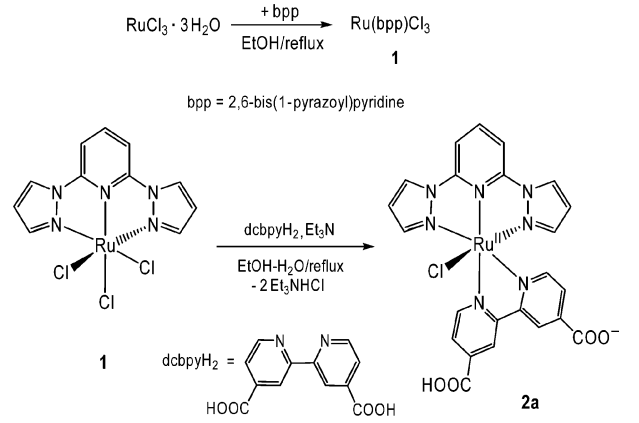

Scheme 2. Stepwise formation of complexes **1**, **2a**.

In a boiling methanol/water solution (1:1, v/v) containing an excess of the amphidentate thiocyanate ligand, complex **2a** undergoes metathesis reaction resulting in the isothiocyanato complex [Ru(bpp)(dcbpyH)(NCS)] (**3**), that was isolated as an orange-red solid in 89% yield [Equation (1)]. This complex shows a remarkable thermal stability and decomposes without melting at 261–262 °C.

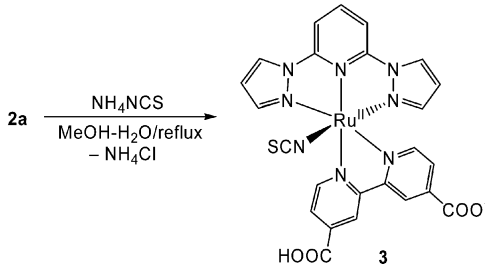

(1)

Monitoring of the reaction by FT-IR and ^1H NMR spectroscopy revealed that the reaction was completed after 4 h of heating. Elemental analysis data for complexes **2a** and **3** are consistent with the calculated composition of the proposed structure. This is also supported by FT-IR spectroscopy (see corresponding section concerning IR spectroscopy) and by derivatization, i.e. formation of the $[Ru(bpp)(dcbpyH_2)Cl]Cl$ complex (**2b**), where both carboxylate groups are protonated (vide infra).

In addition, compound **2a** reacts in the presence of an excess of NaCN, under the same conditions, to give the cyano complex Na[Ru(bpp)(dcbpy)(CN)] (**4**) as an orange solid in 67.5% yield [Equation (2)]. Complex **4** decomposes upon melting at 249 °C.

Addition of an aqueous solution of HCl (excess), to **2a** is accompanied by protonation of the carboxylate ($–COO^-$) group of the bidentate ligand (dcbpyH), affording quantitatively the $[Ru(bpp)(dcbpyH_2)Cl]Cl$ dye (**2b**), as a brown-black solid [Equation (3)].[17] It is a stable solid that does not decompose after heating at 240 °C.

Following a simple purification step, i.e. crystallization of the crude products, all complexes have been obtained in high yield as air stable and analytically pure solids. Therefore, the use of time-consuming column chromatography

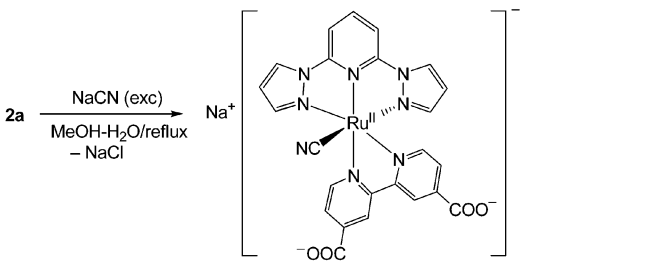

(2)

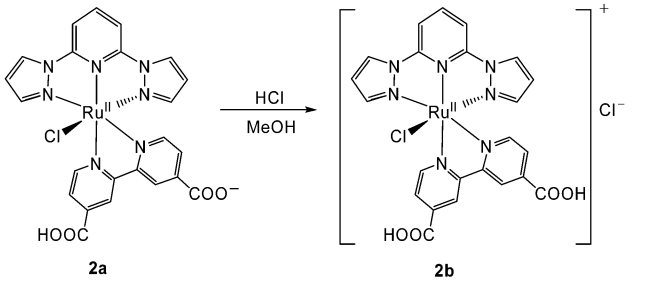

(3)

purification is avoided. In addition, in the case of complex **3**, only the N-bonded isomer was isolated (see IR-Raman section).[18] This is very important, since ruthenium bipyridine complexes with thiocyanate ligands typically yield an isomeric mixture of N- and S-bonded isomers.[15,19] Compounds **2**–**3** were found to be soluble in dimethylformamide (DMF), dimethyl sulfoxide (DMSO), and slightly soluble in methanol. The corresponding complex **4** dissolves very well in water and is less soluble in DMSO. The composition of the ruthenium(II) complexes **2a**–**4** was confirmed by elemental analyses and their spectroscopic properties were examined by FT-IR, FT-Raman, UV/Vis and ^1H NMR spectroscopy. The molecular composition of all compounds was further confirmed by mass spectrometric data (electrospray). The molecular structure of **4**·7.5H_2O·0.5CH_3CN was determined by single-crystal X-ray diffraction (vide infra). Also the corresponding [Ru(bdmpp)(dcbpyH_2)Cl]-(PF_6) sensitizer **5**[13b] was characterized by X-ray crystallography and the crystallographic data were compared with those of **4**.

Characterization

IR-Raman Spectroscopic Data

The IR spectra of complexes **2a** and **3** are almost identical in the region of 4000–400 cm^{-1} as expected for isostructural compounds, except for the presence of a strong NCS band (in complex **3**) at 2109 cm^{-1} which is assigned to the ν_{as}(NCS) mode. This band appears at a position close to that of related ruthenium(II) complexes for which N-bonding of the NCS group has been confirmed.[20] The presence of a less intense band at 815 cm^{-1} is assigned to the ν_s(C=S) stretching vibration.[21] The Raman band that is characteristic of the ν_{as}(NCS) vibration appears at 2112 cm^{-1}, slightly shifted compared to the value observed by IR spectroscopy (Table 1). Both complexes exhibited a broad and medium intensity absorption band at 1718 and 1717 cm^{-1} respectively which is assigned to the ν(C=O) stretching vibration. This band has a slightly higher frequency than that of [Ru(bdmpp)(dcbpyH_2)Cl](PF_6) (1715 cm^{-1})[13b] and [Ru(bdmpp)(dcbpyH_2)(NCS)](PF_6) (1713 cm^{-1}) respectively[13a] which may be attributed to the higher electron density at the Ru^{II} center of complexes bearing the methyl-substituted pyrazolyl-pyridine ligand bdmpp. The bands at 1628 and 1627 cm^{-1} respectively, overlapping with the bpy bands[3c,19] at 1609 and 1610 cm^{-1}, are tentatively assigned to the antisymmetric carboxylate vibration $\nu_{as}(CO_2^-)$.[22] The cationic complex **2b** displays the ν(C=O) stretching vibration at 1718 cm^{-1}, while the ν(C–O) mode is present as a medium intensity band at 1230 cm^{-1}.[5a]

The absence of IR bands above 1700 cm^{-1} in the anionic complex **4** indicates that no protonated C=O group is present. Instead, there is a very strong and broad band at 1600 cm^{-1} which is assigned to the antisymmetric stretching vibration of $\nu_{as}(CO_2^-)$. The strong band at 1377 cm^{-1} can probably be assigned to the symmetric vibration mode $\nu_s(CO_2^-)$ of the carboxylate group.[23] The presence of a terminal cyanido ligand in **4** is indicated by a medium intensity ν(CN) IR absorption band at 2077 cm^{-1} and thus corroborates the molecular structure of **4** determined by X-ray crystallography (vide infra). This band appears at a position close to that of the cyanide ion in NaCN (ν(CN) = 2085 cm^{-1}). The ν(CN) frequency of **4** is comparable with those of similar ruthenium complexes Na_4[Ru(dcbpy)$_2$-(CN)$_2$] (2077 and 2059 cm^{-1}),[24] [Ru(ttp)(L)(CN)](PF_6)[25]

Table 1. Selected Raman and FT-IR spectroscopic data [cm^{-1}] of complexes **2**–**4**.

Complexes	ν(N=C)	ν(C=O)	$\nu_{as}(CO_2)$	ν(C=C)	ν(C=C)	ν(C=N)	$\nu_s(CO_2^-)$	ν(C–O)
2a (IR)	–	1718 (m)	1628 (m)[a]	1609 (s)	1539 (m)	1481 (vs)	1369 (m)	1237 (m)
(Raman)	–	–	–	1612	–	–	1368	–
2b (IR)	–	1718 (m)	–	1610 (s)	1539 (m)	1483 (vs)	–	1230 (m)
(Raman)	–	1718 (m)	–	1612	–	–	–	1224 (w)
3 (IR)	2109 (vs)	1717 (m)	1627 (m)[a]	1610 (s)	1543 (m)	1482 (vs)	1371 (m)	1233 (m)
(Raman)	2122 (s)	–	–	1613	–	–	–	–
4 (IR)	2077 (m)	–	1600 (vs)	–	1543 (m)	1479 (vs)	1377 (m)	1234 (w)
(Raman)	2076 (w)	–	1610 (vs)	–	1542 (m)	1476 (m)	1367 (vs)	1226 (m)

[a] The IR bands at 1628 and 1627 cm^{-1}, overlap with that of the bpy ring modes ν(C=C) at 1609 and 1610 cm^{-1}.

[ttp = 4′-p-tolyl-2,2′:6′,2′′-terpyridine, L = bpy, ν(CN) = 2079 cm^{-1}; L = Phen, ν(CN) = 2075 cm^{-1}], and *cis*-[(Et_2-dcbpy)$_2$Ru(CN)$_2$] [ν(CN) = 2085 and 1996 cm^{-1}], respectively.[26] Also it compares well with the stretching vibration of the osmium complex [Os(H_2teterpy)(CN)$_3$](TBA)$_2$ [ν(CN) = 2076 cm^{-1}, H_3teterpy = 2,2′:6′,2′′-terpyridine-4,4′,4′′-tricarboxylic acid, TBA = tetrabutylammonium].[27] In addition, the Raman spectrum of complex **4** in crystalline form gave very well resolved bands indicative of the high purity of this material, confirming the presence of the characteristic ν(CN) mode as a medium intensity band at 2076 cm^{-1}.

Moreover, the Raman spectrum of **2b** reveals at low frequency a medium intensity band for the ν_s(Ru–Cl) stretching mode at 335 cm^{-1}. This value compares well with that mentioned for [$RuCl_4$(MeCN)$_2$](NEt_4).[28]

NMR Spectroscopic Studies

The ^{1}H NMR spectra of all complexes show a similar pattern in the aromatic region, indicating that substitution of the chlorido ligand by pseudohalides takes place without significant changes in the octahedral geometry at the ruthenium atom. In all cases signal assignment is based on integration, splitting patterns, chemical shifts, ^{1}H-^{1}H COSY experiments, and literature values concerning similar systems.[13,16]

The ^{1}H NMR spectra of complexes **2**–**4** were recorded in $(CD_3)_2SO$ at ambient temperature and Figure 1 presents the characteristic spectrum of complex **2a**. In this solvent, the compound **2a** undergoes substitution of the chlorido ligand, because of its labile nature,[29] as evidenced in the ^{1}H NMR spectrum of **2a** which shows the formation of new resonance signals next to the expected ones, after 14 h standing. For this reason, only data from freshly prepared samples provides a basis for proper interpretation. The aromatic region of the spectrum of complex **2a** displays six sharp (four doublets and two singlets) and well-resolved resonance signals at δ = 10.09 (H^{21}), 9.26 (H^{18}), 9.01 (H^{15}), 8.25 (H^{20}), 7.53 (H^{12}), and 7.35 (H^{13}) ppm respectively, attributable to the six protons of the 2,2′-bipyridine-4,4′-dicarboxylic acid ligand. In addition, the ^{1}H NMR spectrum of **2a**, shows a multiplet signal at δ = 8.45 ppm for the three pyridyl hydrogen atoms (C_6H_3 moiety, H$^{5-7}$). Two doublet signals at δ = 9.28 (H^{1,11}), 7.40 (H^{3,9}) ppm and a pseudotriplet resonance at δ = 6.70 ppm (H^{2,10}) are due to the chemical equivalent pyrazolyl hydrogen atoms.

The low field singlet at δ = 10.09 ppm is assigned to the H^{21} proton of dcbpyH that is close to the coordinated chlorine atom. This singlet signal is upfield shifted by 0.55 and 0.29 ppm respectively, compared to the isothiocyanato complex **3** and the cyano complex **4**. Both the H^{18} and H^{15} singlet resonances of complexes **3** and **4** are shifted upfield compared to the precursor (**2a**) by 0.22 (0.46) and 0.21 (0.39) ppm, respectively.

Electronic Spectra

The UV/Vis absorption spectra of freshly prepared complexes **2**–**4** measured in DMSO are shown in Figure 2 and the corresponding electronic spectroscopic data are summarized in Table 2.

The high energy bands in the 294 to 313 nm range are assigned to π-π* charge-transfer transitions localized on bipyridine ligands.[30] The absorption bands in the visible region can be assigned to the metal-to-ligand charge transfer transition bands (^{1}MLCT), as mentioned for other Ru^{II} polypyridyl complexes.[31] The UV/Vis spectra of **2** and **3** are similar displaying a broad band that consists of three absorption bands in the visible region at 480, 434, 384 (**2a**),

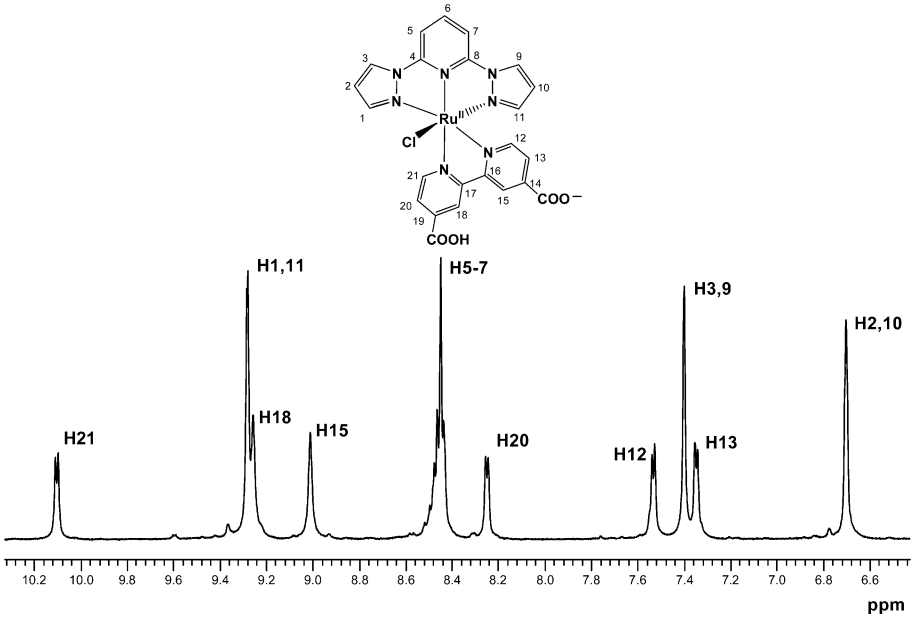

Figure 1. ^{1}H NMR spectrum of complex [Ru(bpp)(dcbpyH)Cl] (**2a**) in $(CD_3)_2SO$ at ambient temperature. A numbering scheme showing our tentative assignment for NMR peaks is included.

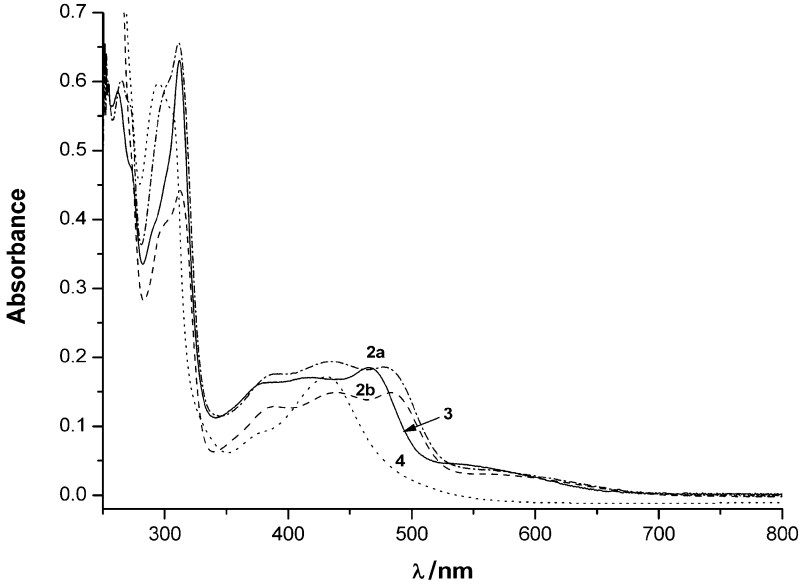

Figure 2. UV/Vis absorption spectra of **2a** (-.-), **2b** (···), **3** (—), and **4** (---) in dimethyl sulfoxide at 298 K.

Table 2. Electronic spectroscopic data of the complexes **2**–**4** measured in DMSO solution at 289 K.

Complexes	Absorption data [λ_{max} [nm] (ε, 10^3 M^{-1} cm^{-1})]			
2a	312 (25.5)	384 (6.8)	434 (7.3)	480 (7.5)
2b	313 (49.9)	388 (14.6)	438 (16.8)	483 (16.8)
3	312 (29.4)	376 (7.5)	418 (7.9)	466 (8.6)
4	307 (11.5)	–	377 (1.9)	430 (3.6)

483, 438, 388 (**2b**), and 466, 418, 376 (**3**) nm, respectively. The visible spectrum of sensitizer **4** displays a broad band at 430 nm. The complexes **2a**, **3**, **4** maximum absorption wavelengths are blue shifted in the order Cl^-, NCS^-, CN^-, consistent with a decrease of electron density on the metal, as previously reported for ruthenium(II) dyes.[32] It is also worth mentioning that the absorption spectra of **2a**, **2b**, and **3** show a broad band at approximately 570 nm (530 nm for **3**), that expands in the near-IR region, up to 700 nm (approximately 610 nm for **3**). This behavior is very important for the photosensitization process as it permits harvesting and transformation of the less energetic photons.[10a] On the other hand, the ^{1}MLCT bands of the cationic complex **2b** with fully protonated –COOH groups in the bipyridine ligand are slightly shifted toward the red compared to **2a** (from 480, 433, and 384 nm to 483, 438, and 388 nm).[33] It has to be mentioned that comparing complexes **2a** and **2b,** the extinction coefficient increases significantly. This behavior has also been verified by recording the spectra of the two dyes in amine-free dimethylformamide solution, where a similar increase of the extinction coefficient (ε) by about 25% was observed. This can be attributed to the different structure of the two complexes (**2a** is an internal salt while **2b** is a typical inorganic salt). In addition, for both complexes in DMF, a hypsochromic shift was observed (λ_{max} = 456 nm for **2a** and λ_{max} = 468 nm for **2b**). Finally, detailed analysis has shown that our complexes present no emission at ambient temperature in DMSO (**2a**–**3**) and aqueous solutions (**4**), respectively. The same result was confirmed with degassed solvents. Additionally, no emission signal was observed for dyes **2a**–**3** chemically attached on the surface of TiO_2 films. Indeed, emissive ruthenium(II) complexes incorporating the 2,6-bis(1-pyrazolyl)pyridine ligand have not been reported to date. This is mainly attributed to the fact that these complexes are expected to have low-lying triplet ligand field excited states (^{3}LF) that facilitate rapid nonradiative decay therefore decreasing the probability of radiative emission.[34] On the contrary luminescent complexes with terpy ligands of the type $[Ru(terpy)(bpy)L]^{2+}$ are well known, which are generally weak emitters at room temperature.[35] Accordingly, no room-temperature emission was observed for the *cis*-[2,2′-bipyridine-5,5′-$(CO_2H)_2$]$_2$Ru$(X)_2$ (X = Cl^-, CN^-, NCS^-) complexes.[36]

X-ray Diffraction Studies

The solid-state structure of complex **4** was determined by single-crystal X-ray diffraction. For comparison reasons, the molecular structure of its analogue, the Ru^{II} complex $[Ru(bdmpp)(dcbpyH_2)Cl](PF_6)$ (**5**), is described. The molecular structures of **4** and **5** are depicted in Figures 3 and 4, respectively.

Both complexes reveal distorted octahedral geometry around the ruthenium metal ion. Distortion results from the constrained bite angle of the chelating tridentate of 156.15(3)° and 156.5(3)° for N(1)–Ru–N(5), respectively. Also deviation from an octahedral geometry is evidenced from the short bite angle N(11)–Ru–N(12) of 77.68°(12) and 78.6°(3), respectively, as observed in [Ru(bdmpp)-(bpy)Cl]Cl·1.25$CHCl_3$,[37] [N(11)–Ru–N(21) 79.8°(5)], and in *cis*-$[Ru(dcbpyH_2)_2(NCS)_2]$·5.0DMSO,[38] [N(11)–Ru–N(21) 79.8°(5), N(31)–Ru–N(41) 79.1°(5)]. As a result of the constrained bite angle of the 2,6-bis(1-pyrazolyl)pyridine ligands, the ruthenium–nitrogen bond to the pyridine nitrogen [complex **4**, Ru–N(3) 1.987(3) Å; complex **5**,

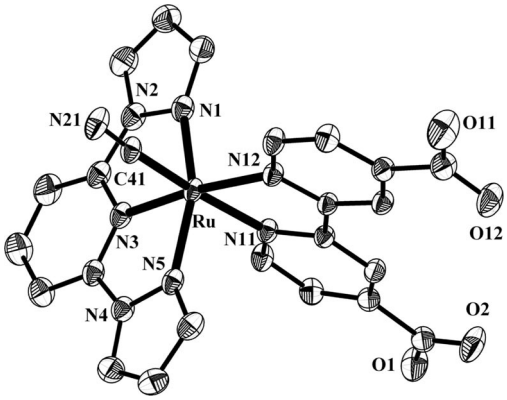

Figure 3. A perspective view of the anion **4**·7.5H_2O·0.5CH_3CN in the solid state. Thermal ellipsoids are set at the 50% probability level. Hydrogen atoms and solvate (water and acetonitrile) molecules have been omitted for clarity. Selected bond lengths [Å] and bond angles [°] of **4**·7.5H_2O·0.5CH_3CN: Ru–N(1) 2.096(4), Ru–N(3) 1.987(3), Ru–N(5) 2.061(4), Ru–N(11) 2.109(3), Ru–N(12) 2.080(3), Ru–C(41) 1.999(4), N(1)–Ru–N(3) 77.8(14), N(1)–Ru–N(11) 95.0(13), N(1)–Ru–N(12) 106.6(13), Ru–C(41)–N(21) 176.1(4).

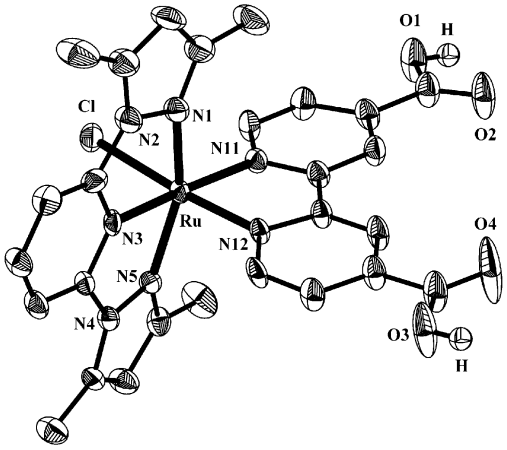

Figure 4. A perspective view of the cation **5**·2CH_3CN·0.5CH_3OH (50% probability of thermal ellipsoids). Hydrogen atoms on the carboxylate moieties of the dcbpyH_2 are shown only. The remaining H-atoms and the solvate (water and acetonitrile) molecules have been omitted for clarity. Selected bond lengths [Å] and bond angles [°] of **5**·2CH_3CN·0.5CH_3OH: Ru–N(1) 2.086(8), Ru–N(3) 1.987(7), Ru–N(5) 2.069(7), Ru–N(11) 2.065(7), Ru–N(12) 2.024(7), Ru–Cl 2.403(3), N(1)–Ru–N(3) 79.0(3), N(1)–Ru–N(11) 99.5(3), N(12)–Ru–Cl 174.9(2), N(1)–Ru–Cl 86.9(2).

1.987(6) Å] is shorter than those belonging to the pyrazolyl substituents [complex **4**, Ru–N(1) 2.096(4) Å, Ru–N(5) 2.061(4) Å; complex **5**, 2.085(8) Å, 2.096(4) Å]. The ligands bpp and bdmpp chelate meridionally via the three nitrogen atoms, i.e. N(1), N(3), and N(5), forming a plane with one nitrogen [N(12) or N(11), respectively] of the functionalized 2,2′-bipyridine ligand. The second nitrogen atom [N(11) or N(12), respectively] of the dcbpyH_2 and the chlorido (cyanido) ligand occupies the axial positions. The Ru–Cl bond length of **5**·2CH_3CN·0.5CH_3OH [2.403(2) Å] lies in the expected range for related Ru^{II} complexes, [Ru(bdmpp)(bpy)Cl]Cl·1.25$CHCl_3$, [Ru–Cl 2.419(3) Å],[37] [Ru(bdmpp)(Me_2bpy)Cl](PF_6)·1.25$CHCl_3$ [Ru–Cl 2.445(2) Å],[37] [Ru(dcbpyH_2)(cymene)Cl][NO_3] [Ru–Cl 2.3966(10) Å].[34] Likewise, the Ru–C41 bond length of the cyanido ligand in **4**·7.5H_2O·0.5CH_3CN [1.999(4) Å] lies in the range observed for other anionic [Ru(CN)(py)(pc)](NBu_4) [pc = phthalocyanine, Ru–C 2.01(2) Å],[39] and cationic ruthenium cyano complexes [Ru(terpy)(phen)(CN)](PF_6) [Ru–C 2.004(3) Å].[40] The coordination geometry around the Na^+ cation is distorted octahedron comprised of water solvate molecules, whereas no interactions less than 3 Å are observed between the Na^+ and the oxygen atoms of the carboxylate groups. The separations of the oxygen atoms of the water molecules to the Na^+ cation lay in the range 2.249(9)–2.968(26) Å. In the structure of **4**, intermolecular distances in the range 2.752–3.268 Å between the solvate water molecules and the carboxylato oxygen atoms as well as the cyano nitrogen atom, result in an interesting hydrogen-bonding pattern, which contributes to the further stability of the lattice structure. The cations of **5** are doubly hydrogen bonded through the protonated carboxylate moieties of the dcbpyH_2 ligand giving rise to the formation of dimers [HO3···O2′ (1 – *x*, –*y*, 1 – *z*) 1.905 Å, O3···O2′ 2.698 Å, O3–HO3···O2′ 162.5°].

Electrochemistry

The cyclic voltammograms were recorded in ca. 10^{-3} M aqueous solutions of the corresponding complexes using 0.1 M NBu_4ClO_4 as a supporting electrolyte, at a sweep rate of 100 mV s^{-1}. Well-defined reversible oxidation/reduction waves were obtained attributed to the Ru^{II}/Ru^{III} redox couple. It has been observed that the cationic dye (**2b**) has higher oxidation potential (+0.73 vs. Ag/AgCl) than the neutral (**2a**) one (+0.68 vs. Ag/AgCl). Taking into account that the onset of the dye absorption spectra is the same, this implies that in the case of TiO_2 sensitization the energetic diagrams of the corresponding interfaces are different and therefore electron injection yield is expected to be larger for complex **2b** compared to **2a**.[50b]

Photovoltaic Performance

The absorption spectra of the new dyes on TiO_2 films (after subtraction of background absorption from the TiO_2 and conductive glass) are shown in Figure 5. The absorption peaks for the chemisorbed dyes **2a**–**3** are all quite broad, compared with the corresponding dye peaks in dimethyl sulfoxide solution. It is easily observed that the absorption intensity of dye **2b** on the TiO_2 film is higher than that of **2a**, indicating that this complex is more efficiently adsorbed on the TiO_2 surface than **2a**. In fact, the amount of adsorbed dye to the surface of the TiO_2 films was determined by desorbing the dye from the TiO_2 surface into a 0.001 M NaOH aqueous solution. The number of adsorbed molecules of the dye adsorbed per square centimeter of geometrical surface area (Γ) for the four dyes **2a**–**4** is listed in Table 3. The Γ value for dye **2b** was determined to be 1.6×10^{-7} mol cm^2, which is about an order of magnitude higher than that for dye **2a** (5.9×10^{-8} mol cm^2). Therefore, upon sensitization, significant differences in J_{sc} between the

two dyes are expected. The increased dye uptake in the case of a solar cell sensitized with dye **2b** (the Γ value of **2b** is almost the same as that of N719[41]) results in increased short circuit photocurrent density (J_{sc}), mainly responsible for the higher conversion efficiency of complex **2b**. In fact, the J_{sc} value of the **2b**-sensitized solar cell was about two times higher than that of the **2a**-sensitized solar cell, which was expected from the UV/Vis spectra. The low efficiency of dyes **2a**, **3**, and **4** is correlated with the lower absorption coefficient of these dyes (Table 2 and Figure 5) and/or to the decreased amount of dye molecules on the titania surface (Table 3).

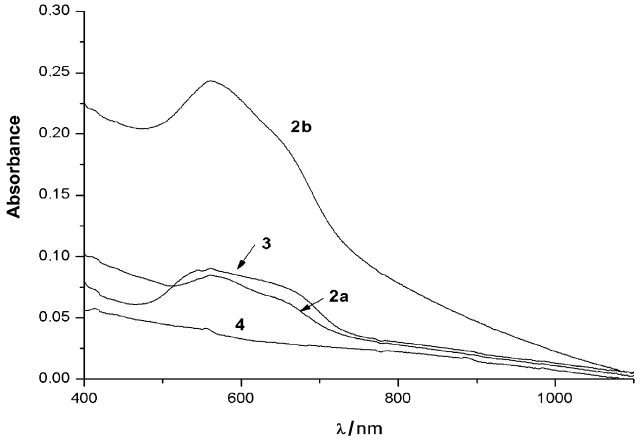

Figure 5. Absorption spectra of the four dyes **2**–**4** on TiO_2 electrodes.

Table 3. Photovoltaic performance (under standard AM 1.5 illumination conditions) of solid-state DSSCs using the Ru^{II} dyes **2**–**5** and a PEO/TiO_2/I^-/I_3^- composite polymer redox electrolyte [corresponding parameters: short circuit photocurrent density (J_{sc}); open circuit potential (V_{oc}); fill factor (*ff*) and power conversion efficiency (η), using the N719 dye are also given]. Surface concentration (Γ) of the chemisorbed dyes is also included.

Dyes	J_{sc} [mA cm^2]	V_{oc} [mV]	*ff*	η [%]	Γ [mol cm^2]
2a	1.56	541	0.58	0.49	5.9×10^{-8}
2b	3.32	580	0.58	1.12	1.6×10^{-7}
3	1.88	545	0.54	0.55	2.0×10^{-8}
4	1.46	532	0.58	0.45	7.0×10^{-9}
5	4.025	493	0.56	1.11	–
N719	9.29	583	0.53	2.87	1.6×10^{-7}

The titania thin films (deposited on conductive glass substrates) were sensitized at ambient temperature for 12–15 h by immersing them into a c.a. 3×10^{-4} M solution of the complexes in DMSO. To evaluate their sensitizing ability and compare their photovoltaic performance, the complexes **2**–**4** chemically attached on the titania electrodes, were incorporated in sandwich-type solid-state solar cells employing a composite polymer redox electrolyte (PEO/TiO_2/I^-/I_3^-) (PEO = polyethylene oxide, MW = 2×10^6)[14] and using a platinized TEC 8 counter electrode. The *cis*-[Ru(dcbpyH)$_2$(NCS)$_2$](NBu$_4$)$_2$ (**N719** dye, purchased from Solaronix) was used as a standard to compare the new sensitizers. Typical photocurrent-density photovoltage curves of DSSCs with the ruthenium dyes **2**–**4** (obtained at AM 1.5 simulated solar irradiation) are shown in Figure 6 and the relevant parameters are summarized in Table 3.

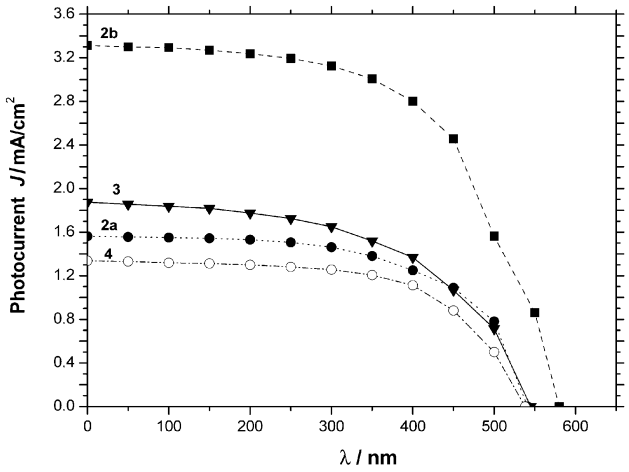

Figure 6. Photocurrent density–photovoltage characteristics of DSSCs using the Ru^{II} dyes **2a** (---●---), **2b** (---■---), **3** (—◀—) and **4** (---○---) under AM 1.5 simulated light.

Under standard global AM 1.5 illumination conditions, solar cells of dye **2b** gave a short-circuit photocurrent density (J_{sc}) of 3.32 mA cm^2, 580 mV open circuit potential (V_{oc}), and 0.58 fill factor (*ff*) yielding an overall power conversion efficiency (η) of 1.12%. Under similar experimental conditions, the **2a** dye produces lower (1.56 mA cm^2) short-circuit current density and open circuit potential of 541 mV, respectively. The open-circuit voltage of **2b** is similar to that of the **N719** dye and by 8% larger than that of **2a**, probably due to the suppression of the dark current.[2a,42] On the other hand, the short-circuit photocurrent density and open circuit voltage of the cells with the cyano complex **4** slightly decrease compared to the precursor **2a**. The observed photovoltaic parameters J_{sc}, V_{oc}, and *ff* (see Table 3) for complex **4** are significantly higher than those of the corresponding *cis*-[Ru(dcbpyH$_2$)(CN)$_2$] sensitizer (1.06 mA cm^2, 310 mV, and 0.24, respectively).[43] Finally, the value of the fill factor (*ff*) is not affected by the nature of the dye, while the overall conversion efficiency is in the 0.5% range for sensitizers **2a**, **3**, and **4**, respectively. It has to be pointed out that in complex **4**, coordination to the Ti^{4+} center on the TiO_2 surface could occur via the lone pair of electrons on the nitrogen of the –CN functional group.[44] In addition, the two deprotonated carboxylate (–COO^-) groups of the complex, appear to be anchored on the semiconductor surface via bidentate or bridging coordination as previously demonstrated for the **N712** dye.[22]

These data clearly indicate that the performance characteristics of complex **2b**, with fully protonated carboxylate groups of the dcbpyH$_2$ ligand, are superior to those of the dyes **2a**–**4**, while the **N719**-sensitized solar cell gave the best overall efficiency. This is further supported by the cyclic voltammetry results. Also the better performance may be attributed to the higher number of protons carried by the sensitizer, something which is in accord with the reports

mentioned for carboxylated Ru^{II} phenanthroline complexes.[45] In fact, complex **2b** contains one more proton compared to **2a** and **3**, and two additional protons from the sensitizer **4**. In addition, the corresponding solid-state solar cell using the dye **2b** shows similar overall energy conversion efficiency (η) compared to that of the methylated derivative [Ru(bdmpp)(dcbpyH$_2$)Cl](PF$_6$).[13b] Further studies are in progress to improve the photovoltaic characteristics of the dye-sensitized solar cell based on heteroleptic complexes including bpp ligands.

Conclusions

Halide substitution reactions of the [Ru(bpp)(dcbpyH)Cl] precursor **2a** with various nucleophiles (NCS^-, CN^-) led straightforwardly to the neutral and anionic sensitizers [Ru(bpp)(dcbpyH)(NCS)] (**3**) and (Na)[Ru(bpp)(dcbpy)(CN)] (**4**), respectively. Also reaction of **2a** with the electrophile (HCl) gave quantitatively the cationic [Ru(bpp)(dcbpyH$_2$)Cl]Cl complex. Following simple purification techniques the isolated dyes are analytically pure and used as such for solar cell applications. All new heteroleptic Ru^{II} compounds have been anchored to nanocrystalline TiO_2-film electrodes using a solid-state electrolyte, namely PEO/TiO_2/I^-/I_3^-, and the photovoltaic properties of the resulting dye-sensitized solar cells have been characterized and compared with the properties of the one prepared with *cis*-[Ru(dcbpyH)$_2$(NCS)$_2$](NBu$_4$)$_2$ (**N719**). The photovoltaic performance of nanocrystalline TiO_2 solar cells sensitized by the complexes **2**–**4** bearing the 2,6-bis(1-pyrazolyl)pyridine and bipyridinedicarboxylic acid depends remarkably on the number of carboxyl functional groups. Thus, the [Ru(bpp)(dcbpyH$_2$)Cl]Cl dye **2b** (with two carboxyl anchoring groups), yields under standard AM 1.5 illumination a 1.12% power conversion efficiency that is about two-times higher than that of the solar cells sensitized with the dyes **2a** and **3** (bearing one carboxy group) and of complex **4** (without any carboxy group). However, dye **2b** is almost 40% less efficient than the **N719**-sensitized solar cell. As expected, the photovoltaic performance of the Ru–NCS dye **3** was higher than that of the Ru–Cl precursor **2a**, and this can be attributed to a better tuning and stabilization of the t_{2g} orbitals of the thiocyanate complex.[13a] We are currently examining the photovoltaic characteristics of all the above dyes in semi-solid propylene carbonate-based modified nanocomposite redox electrolytes prepared in our group. This is expected to lead to cell optimization and a further efficiency increase of the corresponding DSSCs.

Experimental Section

General Procedures and Materials: All manipulations (unless otherwise noted) were carried out under Ar using standard Schlenk techniques. $RuCl_3 \cdot 3H_2O$ and the solvents were used without further purification. The ligand 2,6-bis(1-pyrazolyl)pyridine was prepared according to literature methods.[11] The solvents used were thoroughly degassed by argon passage for 20 min before use. Elemental analyses were obtained from the Central Analytical Group of the Chemistry Department of the Humboldt-Universität zu Berlin. The C, H, N analyses of all compounds were carried out twice on a Leco CHNS-932 elemental analyzer. The mean C, H, N values of each compound are given below. Chlorine was determined using Schöniger's method followed by titration with $Hg(ClO_4)_2$.[46] Melting or decomposition points were determined with a Büchi SMP 530 melting point apparatus (Dr. Tottoli, patent 320338) and were not corrected. The samples were sealed in capillary tubes and heated slowly until the compounds melted or decomposed. Infrared spectra were measured with a Nicolet 550 Magna-IR™ spectrometer as KBr pellets in the region of 4000–400 cm^{-1}. The following abbreviations were used for the intensities of the IR absorption bands: vs. = very strong, s = strong, m = medium, w = weak, sh = shoulder. The solid-state RAMAN spectra were recorded in a frequency range of 3700–3 cm^{-1} (Bruker Vertex 70/RAM II) with an excitation wavelength of 1064 nm, at ambient and low temperature (140 K) applying a laser power of 4–250 mW on the sample. Spectra were an average of 64 or 1024 scans collected at 4 cm^{-1} resolution. Absorption spectra were recorded with a Perkin–Elmer Lambda 19 UV/Vis spectrometer and emission spectra were recorded with a Photon Technology International QM-1 steady-state spectrometer of the School of Chemistry, University of Birmingham. ^1H NMR spectra were measured with a Bruker Avance 500 MHz or a Bruker AM-300 spectrometer in $(CD_3)_2SO$ at the NCSR Demokritos and the Chemistry Department of the Humboldt-Universität zu Berlin. The spectra were calibrated against the residual proton resonances of the deuterated solvent ([D$_6$]DMSO, δ_H = 2.49 ppm). Electrospray mass spectra ESMS-TOF (TOF = time of flight) and ESMS were performed at the Mass Spectrometry Service Centre of the School of Chemistry, University of Birmingham and at the Mass Spectrometry and Dioxin Analysis Lab. IRRP of the National Centre for Scientific Research "Demokritos". Cyclic voltammetry measurements were performed in ca. 10^{-3} M aqueous solutions of the corresponding complexes containing 0.1 M NBu_4ClO_4 as supporting electrolyte, at a sweep rate of 100 mV s^{-1}, using a PAR Model 174 A polarographic analyzer operating in conjunction with a 33120 A Hewlett–Packard function–arbitrary waveform generator. A three-electrode three-compartment electrochemical cell was used, with Metrohm dot (6.0302.000) and planar (6.0305.000) platinum working and counter electrodes, respectively, as well as a Metrohm Ag/AgCl 6.0726.100 reference electrode. The experiments were performed in deoxygenated solutions purified by Ar gas (99.9%) for 30 min prior to use. During the experiment the Ar was passed over the solution surface.

Crystal Structure Determination of 4·7.5H$_2$O·0.5CH$_3$CN, and 5·2CH$_3$CN·0.5CH$_3$OH: Orange prismatic crystals of **4**·7.5H$_2$O·0.5CH$_3$CN were obtained upon slow diffusion of an acetone/acetonitrile mixture (20 mL, 10:1, v/v) into an aqueous solution (3–4 mL) of complex **4** at ambient temperature. Brown prismatic crystals of **5**·2CH$_3$CN·0.5CH$_3$OH were grown upon slow diffusion of diethylether into a solution of **5** in an acetonitrile/acetone mixture (4:1, v/v) at room temperature. Diffraction measurements were taken with a Crystal Logic Dual Goniometer diffractometer using graphite monochromated Mo-K_α radiation. Important crystal data and parameters for data collection are reported in Table 4. Unit cell dimensions were determined and refined by using the angular settings of 25 automatically centered reflections in the range $11° < 2\theta \leq 23°$. Three standard reflections monitored every 97 reflections showed less than 3% intensity fluctuation and no decay. Lorentz, polarization and psi-scan absorption corrections (for **5** only) were applied using Crystal Logic software. The structures were solved by direct methods using SHELXS-86[47] and refined

by full-matrix least-squares techniques on F^2 with SHELXL-97.[48] Further experimental crystallographic details for **4**: $2\theta_{max}$ = 50°, scan speed 5.0° min; scan range 1.6 +$\alpha_1\alpha_2$ separation; reflections collected/unique/used, 6071/5796 [R_{int} = 0.0073]/5796; 502 parameters refined; $(\Delta/\sigma)_{max}$ = 0.009; $(\Delta\rho)_{max}/(\Delta\rho)_{min}$ = 0.927/–0.356 e Å^3; R/R_w (for all data), 0.0500/0.1402. The asymmetric unit in the cell of **4** contains 7.5 molecules of water and 0.5 molecules of acetonitrile. One of the water solvate molecules [Ow(8)] as well as the MeCN were refined with occupation factors fixed to 0.50. Hydrogen atoms were located by difference maps and were refined isotropically. No H-atoms for the solvate molecules were included in the refinement. All non-H atoms were refined anisotropically. Further experimental crystallographic details for **5**: $2\theta_{max}$ = 45.5°, scan speed 1.2° min; scan range 2.2 +$\alpha_1\alpha_2$ separation; reflections collected/unique/used, 5878/5541 [R_{int} = 0.1096]/5541; 486 parameters refined; $(\Delta/\sigma)_{max}$ = 0.000; $(\Delta\rho)_{max}/(\Delta\rho)_{min}$ = 0.937/–0.308 e Å^3; R/R_w (for all data) = 0.1189/0.2352. Hydrogen atoms were introduced at calculated positions as riding on bonded atoms; except those of the solvate molecules, which were not included in the refinement. All non-H atoms were refined anisotropically. The second acetonitrile solvate molecule was refined isotropically, the methanol solvate was refined isotropically with the occupation factor fixed to 0.50.

Table 4. Crystallographic data for **4**·7.5H_2O·0.5CH_3CN and **5**·2CH_3CN·0.5CH_3OH.

	4·7.5H_2O·0.5CH_3CN	**5**·2CH_3CN·0.5CH_3OH
Formula	$C_{25}H_{31.5}N_{8.5}NaO_{11.5}Ru$	$C_{31.5}H_{33}ClF_6N_9O_{4.5}PRu$
Fw	759.15	891.16
Space group	$P\bar{1}$	$P2_1/c$
T [°C]	298	298
λ [Å]	Mo-K_α (0.71073 Å)	Mo-K_α (0.71073 Å)
a [Å]	11.704(4)	19.589(12)
b [Å]	12.200(4)	20.808(14)
c [Å]	13.178(4)	10.404(6)
α [°]	100.10(1)	90
β [°]	09.81(1)	98.921(19)
γ [°]	103.88(1)	90
V [Å^3]	1649.4(9)	4190(4)
Z	2	4
$\rho_{calcd.}$ [g cm^{-3}]	1.529	1.413
μ (Mo-K_α) [mm^{-1}]	0.558	0.548
*R*1[a]	0.0456[b]	0.0785[c]
wR_2[a]	0.1359[b]	0.1991[c]

[a] w = $1/[\sigma^2(F_o^2) + (aP)^2 + bP]$ and $P = (\max)F_o^2,0) + 2F_c^2)/3$; *R*1 = $\Sigma(|F_o| - |F_c|)/\Sigma(|F_o|)$ and $wR_2 = \{\Sigma[w(F_o^2 - F_c^2)^2]/\Sigma[w(F_o^2)^2]\}^{1/2}$. [b] For 5360 reflections with $I > 2\sigma(I)$. [c] For 3779 reflections with $I > 2\sigma(I)$.

TiO_2 Electrode Preparation: Nanoporous TiO_2 thin films (15 μm thick) on conducting glass substrates TEC 8 (purchased from Hartford Glass Co. Inc.) using the doctor blade technique were prepared, as previously reported.[49] An adhesive tape strip on the conductive glass determines the film thickness. These films were sintered in air at 450 °C at a rate of 20 °C min^{-1} for 30 min and were stored in a vacuum desiccator in the dark until required for use. The titania films were sensitized at ambient temperature for 12–15 h by immersing them into a c.a. 3×10^{-4} M solution of the complexes in dimethyl sulfoxide. Immersion of nanocrystalline titania films in the solution of the dyes resulted in strong coloration of the films (in the case of complex **4** a faint yellow coloration was observed). The dye-coated electrodes were taken out of the solution, washed thoroughly with dimethyl sulfoxide and ethanol to remove any loosely adsorbed dye, shortly dried under a stream of dry argon and used as such for photovoltaic measurements. The sensitized TiO_2 thin films were incorporated in a sandwich-type solar cell employing a solid composite electrolyte ($PEO/TiO_2/I^-/I_3^-$)[14] and using a platinized TEC 8 counter electrode. An adhesive tape was placed between the electrodes to avoid short-circuiting, and the two electrodes were firmly pressed. A more detailed fabrication procedure for the nanocrystalline titania electrodes, the cell assembly, and the photo-electrochemical characterization has been described elsewhere.[50] The working electrode had an illuminated surface of 0.16 cm^2. Photovoltaic data were measured using a 300-W Xenon lamp that was focused to give 1000 W m^2, the equivalent of one sun at AM 1.5, at the surface of the test cell.

Synthesis of [Ru(bpp)Cl_3] (1): A Schlenk tube was charged with 0.165 g (0.63 mmol) of $RuCl_3 \cdot 3H_2O$ and 0.106 g (0.502 mmol) of the bpp ligand and the mixture was degassed by applying fine vacuum for 0.5 h. EtOH (20 mL) was then added to the mixture via a double-ended needle, and the brown suspension was heated to a gentle reflux for 3 h. The resulting red-brown suspension was cooled to ambient temperature and left to settle overnight at 5 °C. The solid precipitated was filtered in air washed with EtOH (3×20 mL) and Et_2O (2×10 mL) and dried in vacuo over P_2O_5 to give complex **1** as a dark red-brown solid; yield 0.21 g (85.2%). **1·4H_2O** $C_{11}H_{17}Cl_3N_5O_4Ru$ (490.72): calcd. C 26.92, H 3.49, N 14.27; found C 26.73, H 3.24, N 13.82. IR (KBr): $\tilde{\nu}$ = 3159 (w, C–H, aromatic), 3124 (w, C–H, aromatic), 3090 (m, C–H, aromatic), 3049 (m, C–H, aromatic), 1576 (w), 1529 (m), 1483 (s), 1433 (w), 1408 (w), 1369 (w), 1346 (s), 1317 (w), 1256 (w), 1194 (w), 1175 (w), 1051 (m), 961 (m), 907 (w), 802 (s), 781 (s, sh), 773 (s, sh), 690 (w), 594 (w), 457 [br. (m)] cm^{-1}.

Synthesis of [Ru(bpp)(dcbpyH)Cl] (2a): Under a slow stream of argon a Schlenk tube was charged with complex (**1**) (0.196 g, 0.399 mmol) and a slight excess of the ligand $dcbpyH_2$ (0.114 g, 0.468 mmol) in an EtOH/H_2O mixture (30 mL, 1:1, v/v) giving a dark brown suspension. LiCl (25 mg, 0.59 mmol) in an EtOH/H_2O mixture (10 mL, 1:1, v/v) and Et_3N (0.11 mL, 0.788 mmol) were added affording instantly a green solution that gradually turned to orange-brown upon heating to a gentle reflux for 7 h. While hot the suspension was filtered (in air) through a pad of Celite. The resulting clear orange-brown solution was concentrated to a few milliliters and was stored for 2 d at 5 °C. The solid precipitated was filtered, washed with small amounts of cold water, Et_2O (15 mL), dried in air and finally in vacuo in a desiccator over P_2O_5. A further crop was obtained from the filtrate upon concentration and storage at 5 °C. This procedure was repeated twice in order to obtain complex **2a** analytically pure as a red-brown microcrystalline solid; yield 0.243 g (97.1%), m.p. >215 °C. **2a·2H_2O**, $C_{23}H_{20}ClN_7O_6Ru$ (626.98): calcd. C 44.06, H 3.22, Cl 5.65, N 15.64; found C 43.90, H 2.96, Cl 5.75, N 15.69. IR (KBr): $\tilde{\nu}$ = 3112 (w, C–H, aromatic), 3089 (m, C–H, aromatic), 3035 (w, C–H, aromatic), 2924 (w, C–H, aliphatic), 1718 [m, ν(C=O)], 1628 [m, $\nu_{as}(CO_2^-)$], 1609 [s, ν(C=C)], 1573 (w), 1539 [m, ν(C=C)], 1521 (w), 1482 [vs, ν(C=N)], 1408 (s), 1369 [m, $\nu_s(CO_2^-)$], 1340 (m), 1306 (w), 1265 (m), 1237 [m, ν(C–O)], 1174 (w), 1129 (w), 1072 (w), 1049 (m), 1025 (m), 955 (m), 901 (m), 774 (s), 717 (w), 684 (m), 595 (w), 528 (w), 445 (m) cm^{-1}. Raman: not possible. ^{1}H NMR [$(CD_3)_2SO$, 500 MHz, 298 K]: δ = 6.70 (br. s, 2 H, 2,10-H), 7.35 (dd, $^3J_{H,H}$ = 5.7 Hz, 1 H, 13-H), 7.40 (br. s, 2 H, 3,9-H), 7.53 (d, $^3J_{H,H}$ = 6.0 Hz, 1 H, 12-H), 8.25 (d, $^3J_{H,H}$ = 5.5 Hz, 1 H, 20-H), 8.45 (m, 3 H, 5–7-H), 9.01 (s, 1 H, 15-H), 9.26 (s, 1 H, 18-H), 9.28 (br. s, 2 H, 1,11-H), 10.09 (d, $^3J_{H,H}$ = 5.6 Hz, 1 H, 21-H) ppm. UV/Vis (ε, M^{-1} cm^{-1}): λ_{max} [$(CH_3)_2SO$] = 480 (7521), 434 (7276), 384 (sh) (6770), 312 (25510) nm; no emission [$(CH_3)_2SO$]. ESMS-TOF (MeOH): *m*/*z* (%) = 592 {M + H}$^+$.

Synthesis of [Ru(bpp)(dcbpyH$_2$)Cl]Cl (2b): 0.25 mL (0.5 mmol) of an aqueous HCl solution (2 M) was added whilst stirring to a suspension of complex (**2a**) (30 mg, 0.051 mmol) in MeOH (10 mL). Immediately, the solid dissolved and the resulting dark red-brown solution was stirred at ambient temperature for 2 h. The volume of the solution was concentrated to some milliliters, and the product was precipitated with diethyl ether (excess). The resulting brown-black solid was washed with Et_2O (2 × 10 mL) and dried in an oven at 50 °C over 2 h; yield quantitative, m.p. >240 °C. **2b·4H$_2$O**, $C_{23}H_{25}Cl_2N_7O_8Ru$ (699.46): calcd. C 39.49, H 3.60, Cl 10.14, N 14.02; found C 39.10, H 3.81, Cl 10.01, N 13.87. IR (KBr): $\tilde{\nu}$ = 3128 (w, C–H, aromatic), 3094 (m, C–H, aromatic), 3071 (w, C–H, aromatic), 2924 (w, C–H, aliphatic), 2851 (w, C–H, aliphatic), 1718 [m, ν_{as}(C=O)], 1610 [m, ν(C=C)], 1572 (br. s), 1547 (br. s), 1539 [m, ν(C=C)], 1520 (br. vs), 1506 (br. s), 1491 (br. s), 1483 [vs, ν(C=N)], 1408 (s), 1367 (w), 1340 (w), 1310 (w), 1258 (m), 1230 [m, ν(C–O)], 1173 (w), 1140 (w), 1126 (w), 1042 (w), 1024 (m), 959 (m), 901 (m), 781 (m), 770 (m), 685 (m), 663 (w), 594 (w) cm^{-1}. Raman [5 mW, r.t., 1024 scans]: 1718 [m, ν_{as}(C=O)], 1612 [m, ν(C=C)], 1575 (m), 1559 (m), 1543 (m), 1498 (w), 1471 (m), 1445 (w), 1414 (w), 1372 (m), 1346 (w), 1310 (w), 1295 (w), 1285 (w), 1265 (m), 1241 (w), 1224 [w, ν(C-O)], 1211 (w), 1188 (w), 1046 (m), 1029 (s), 750 (m), 652 (w), 450 (w), 427 (w), 335 [s, ν_s(Ru-Cl)] cm^{-1}. ^{1}H NMR [(CD$_3$)$_2$SO, 500 MHz, 298 K]: δ = 6.63 (br. s, 2 H, 2,10-H), 7.30 (m, 2 H, 3,9-H), 7.41 (d, $^3J_{H,H}$ = 5.7 Hz, 1 H, 13-H), 7.69 (d, $^3J_{H,H}$ = 5.7 Hz, 1 H, 12-H), 8.30 (m, 4 H, 5- to 7-H + 20-H), 8.80 (br. s, 1 H, 15-H), 9.04 (br. s, 1 H, 18-H), 9.07 (br. s, 2 H, 1,11-H), 10.13 (d, $^3J_{H,H}$ = 5.7 Hz, 1 H, 21-H) ppm. UV/Vis (ε, M^{-1} cm^{-1}): λ_{max} [(CH$_3$)$_2$SO] = 483 (16782), 438 (16782), 388 (sh) (14557), 313 (49871) nm. ESI-MS (MeOH): *m*/*z* (%) = 592 {M + H}$^+$, 556 {M – Cl}$^+$.

Synthesis of [Ru(bpp)(dcbpyH)(NCS)] (3): Under argon a solution of NH_4NCS (0.077 g, 0.873 mmol) in H_2O (5 mL) was added to a solution of complex (**2**) (0.053 g, 0.084 mmol) dissolved in MeOH/H_2O (1:1, v/v) (10 mL). The orange-brown solution was heated to a gentle reflux for 4 h, the resulting orange-red solution was concentrated to a few milliliters and was stored for 2 d at 5 °C. The solid precipitated was filtered off, washed with small amounts of cold water and with Et_2O (20 mL), dried in air and finally in vacuo in a desiccator over P_2O_5. A further crop was obtained from the filtrate upon concentration and storage at 5 °C. This procedure was repeated twice in order to obtain complex **3** analytically pure as an orange-red microcrystalline solid; yield 0.0504 g (89.3%), m.p. 261–262 °C. **3·3H$_2$O**, $C_{24}H_{22}N_8O_7RuS$ (667.62): calcd. C 43.18, H 3.32, Cl 0.00, N 16.78, S 4.80; found C 43.08, H 3.10, Cl 0.41, N 16.73, S 4.50. IR (KBr): $\tilde{\nu}$ = 3146 (w, C–H, aromatic), 3081 (m, C–H, aromatic), 2109 [vs, ν_{as}(NCS)], 1717 [m, ν(C=O)], 1627 [m, ν_{as}(CO_2^-)], 1610 [s, ν(C=C)], 1574 (m), 1543 [m, ν(C=C)], 1522 (w), 1483 [vs, ν(C=N)], 1436 (w), 1405 (s), 1371 [m, ν_s(CO_2^-)], 1344 (m), 1309 (w), 1267 (w), 1233 [m, ν(C–O)], 1174 (w), 1152 (w), 1130 (w), 1076 (w), 1049 (m), 1026 (m), 957 (m), 910 (m), 863 (w), 815 [m, ν_s(NCS)], 774 (s), 756 (s), 719 (w), 706 (w), 681 (m), 665 (w), 598 (w), 528 (w), 463 (w), 445 (w) cm^{-1}. Raman [250 mW, 140 K, 64 scans]: 3046 (m), 2112 [m, ν_{as}(NCS)], 1613 [m, ν(C=C)], 1482 (w), 1434 (w), 1370 (w), 1279 (w), 1069 (w), 1028 (w), 1028 (m), 984 (w), 951 (w), 902 (w), 468 (w) cm^{-1}. ^{1}H NMR [(CD$_3$)$_2$SO, 500 MHz, 298 K]: δ = 6.77 (br. s, 2 H, 2,10-H), 7.38 (d, $^3J_{H,H}$ = 5.0 Hz, 1 H, 13-H), 7.41 (d, $^3J_{H,H}$ = 5.0 Hz, 1 H, 12-H), 7.56 (br. s, 2 H, 3,9-H), 8.29 (d, $^3J_{H,H}$ = 5.0 Hz, 1 H, 20-H), 8.51 (d, $^3J_{H,H}$ = 7.5 Hz, 2 H, 5,7-H), 8.58 (t, $^3J_{H,H}$ = 7.5 Hz, 1 H, 6-H), 8.80 (br. s, 1 H, 15-H), 9.04 (s, 1 H, 18-H), 9.34 (s, 2 H, 1,11-H), 9.54 (d, $^3J_{H,H}$ = 4.50 Hz, 1 H, 21-H) ppm. UV/Vis (ε, M^{-1} cm^{-1}): λ_{max} [(CH$_3$)$_2$SO] = 466 (8591), 418 (7890), 376 (sh) (7540), 312 (29413) nm; small emission [(CH$_3$)$_2$SO]: 667 nm (λ_{exc} = 560 nm). ESMS-TOF (MeOH): *m*/*z* (%) = 659 {M – H + 2Na}$^+$, 637 {M + Na}$^+$, 615 {M + H}$^+$, 586 {M – CO}$^+$, 558 {M – 2CO}$^+$.

Synthesis of Na[Ru(bpp)(dcbpy)(CN)] (4): Under argon a solution of NaCN (0.031 g, 0.63 mmol) in water (5 mL) was added to a solution of complex **2a** (0.034 g, 0.054 mmol) in H_2O/MeOH (1:2, v/v) (15 mL). The orange-brown solution was heated to a gentle reflux for 5 h leading to a clear orange solution that was concentrated to approximately 4–5 mL. Upon addition of acetone (20 mL) an orange solid was precipitated. The latter was filtered off, washed with acetone (2 × 10 mL) and Et_2O (2 × 10 mL) and dried in air as well as in an oven at 70 °C for 0.5 h. X-ray equality orange single crystals of **4**·7.5H$_2$O·0.5CH$_3$CN were obtained upon slow evaporation of a mixture of acetone/acetonitrile (20 mL, 10:1, v/v) into a solution of the product in water. The orange crystals were collected on a filter paper, washed with small amounts of Et_2O (2 × 5 mL) and dried in an oven at 70 °C for 2 h to obtain 22 mg of complex **4**; yield 67.5%, m.p. 249 °C (dec.). **4·6H$_2$O**, $C_{24}H_{27}NaN_8O_{10}Ru$ (711.58): calcd. C 40.51, H 3.82, N 15.75; found C 40.39, H 3.80, N 15.40. IR (KBr): $\tilde{\nu}$ = 3091 (w, C–H, aromatic), 2926 (m, C–H, aromatic), 2852 (w, C–H, aromatic), 2077 [m, ν(CN)], 1600 [vs, ν_{as}(CO_2^-)], 1543 [m, ν(C=C)], 1479 [vs, ν(C=N)], 1431 (vs), 1410 (vs), 1377 [m, ν_s(CO_2^-)], 1342 (m), 1265 (m), 1234 (m), 1177 (w), 1053 (w), 1026 (w), 958 (m), 912 (w), 881 (m), 788 (s), 766 (s), 729 (w), 702 (m), 595 (w), 447 (w) cm^{-1}. Raman [100 mW, room temp., 1024 scans]: 2076 [s, ν(CN)], 1610 [vs, ν_{as}(CO_2^-)], 1576 (w), 1542 (m), 1490 (m), 1476 (m), 1416 (m), 1367 [vs, ν_s(CO_2^-)], 1309 (m), 1289 (m), 1273 (m), 1226 [w, ν(C–O)], 1063 (m), 1045 (s), 1027 (vs), 950 (m), 901 (w), 783 (w), 732 (w), 443 (w), 418 (w), 389 (m), 335 (w) cm^{-1}. ^{1}H NMR [(CD$_3$)$_2$SO, 500 MHz, 298 K]: δ = 6.73 (m, 2 H, 2,10-H), 7.29 (d, $^3J_{H,H}$ = 6.0 Hz, 1 H, 13-H), 7.43 (br. s, 2 H, 3,9-H), 7.45 (d, $^3J_{H,H}$ = 5.0 Hz, 1 H, 12-H), 8.10 (d, $^3J_{H,H}$ = 7.5 Hz, 1 H, 20-H), 8.43 (d, $^3J_{H,H}$ = 7.8 Hz, 1 H, 5,7-H), 8.48 (t, $^3J_{H,H}$ = 8.0 Hz, 1 H, 6-H), 8.65 (br. s, 1 H, 15-H), 8.82 (br. s, 1 H, 18-H), 9.29 (d, $^3J_{H,H}$ = 3.0 Hz, 1 H, 1,11-H), 9.83 (d, $^3J_{H,H}$ = 5.7 Hz, 1 H, 21-H) ppm. UV/Vis (ε, M^{-1} cm^{-1}): λ_{max} [(CH$_3$)$_2$SO] = 430 (3593), 377 (sh) (1880), 307 (11550), 294 (12471) nm. ESMS-TOF (MeOH): *m*/*z* (%) = 649 {M – H + 3Na}$^+$, 627 {M + 2Na}$^+$.

CCDC-639397 (for **4**·7.5H$_2$O·0.5CH$_3$CN) and -639398 (for **5**·2CH$_3$CN·0.5CH$_3$OH) contain supplementary crystallographic data. These data can be obtained free of charge from The Cambridge Crystallographic Data Centre via www.ccdc.cam.ac.uk/data_request/cif.

Acknowledgments

This work has been partially supported by the British Council (Greek-British 2004–2006 bilateral cooperation project), the GSRT Greece (PENED 03EΔ118 project) and the European Union (STREP 033313 project). The authors express their gratitude to Prof. Dr. A. C. Filippou for access to the Central Analytical Group of the Chemistry Department of the Humboldt-Universität zu Berlin and the University of Bonn. Furthermore, we acknowledge Reader Z. Pikramenou and Research Director Dr. L. Leodiadis for access to the Mass Spectrometry Service Centre of the School of Chemistry, University of Birmingham and the Mass Spectrometry and Dioxin Analysis Lab. IRRP of the National Centre for Scientific Research "Demokritos", respectively. Finally, helpful assistance from Dr. G. Pistolis, Dr. E. Chatzivasiloglou, Dr. M. Chatzichristidi, N. Weidemann, G. Konti, and N. Alexaki is highly acknowledged.

[1] a) B. O'Regan, M. Grätzel, *Nature* **1991**, *353*, 737–740; b) M. K. Nazeeruddin, A. Kay, I. Rodicio, R. Humphry-Baker, E. Müller, P. Liska, N. Vlachopoulos, M. Grätzel, *J. Am. Chem. Soc.* **1993**, *115*, 6382–6390; c) M. Grätzel, *Prog. Photovolt. Res. Appl.* **2000**, *8*, 171–185; d) M. Grätzel, *J. Photochem. Photobiol., C* **2003**, *4*, 145–153; e) Z.-S. Wang, H. Kawauchi, T. Kashima, H. Arakawa, *Coord. Chem. Rev.* **2004**, *248*, 1381–1389; f) Md. K. Nazeeruddin, C. Klein, P. Liska, M. Grätzel, *Coord. Chem. Rev.* **2005**, *249*, 1460–1467; g) M. K. Nazeeruddin, F. De Angelis, S. Fantacci, A. Selloni, G. Viscardi, P. Liska, S. Ito, B. Takeru, M. Grätzel, *J. Am. Chem. Soc.* **2005**, *127*, 16835–16847; h) M. K. Nazeeruddin, Q. Wang, L. Cevey, V. Aranyos, P. Liska, E. Figgemeier, C. Klein, N. Hirata, S. Koops, S. A. Haque, J. R. Durrant, A. Hagfeldt, A. B. P. Lever, M. Grätzel, *Inorg. Chem.* **2006**, *45*, 787–797; i) Recently outdoor experiments in Lausanne, Switzerland, under natural sunlight (96 mW cm^2) with the **N719** dye gave an overall conversion efficiency of 12.23%; see: S. Ito, Md. K. Nazeeruddin, P. Liska, P. Comte, R. Charvet, P. Péchy, M. Jirousek, A. Kay, S. M. Zakeeruddin, M. Grätzel, *Prog. Photovolt. Res. Appl.* **2006**, *14*, 589–601; j) N. Robertson, *Angew. Chem. Int. Ed.* **2006**, *45*, 2338–2345; k) J. M. Kroon, N. J. Bakker, H. J. P. Smit, P. Liska, K. R. Thampi, P. Wang, S. M. Zakeeruddin, M. Grätzel, A. Hinsch, S. Hore, U. Würfel, R. Sastrawan, J. R. Durrant, E. Palomares, H. Petterson, T. Gruszecki, J. Walter, K. Skupien, G. E. Tulloch, *Prog. Photovolt. Res. Appl.* **2007**, *15*, 1–18; l) Md. K. Nazeeruddin, T. Bessho, L. Cevey, S. Ito, C. Klein, F. De Angelis, S. Fantacci, P. Comte, P. Liska, H. Imai, M. Graetzel, *J. Photochem. Photobiol., A* **2007**, *185*, 331–337.

[2] a) K. Kalyanasundaram, M. Grätzel, *Coord. Chem. Rev.* **1998**, *177*, 347–414; b) A. Hagfeldt, M. Grätzel, *Acc. Chem. Res.* **2000**, *33*, 269–277; c) M. Grätzel, *Inorg. Chem.* **2005**, *44*, 6841–6851.

[3] a) S. Anderson, E. C. Constable, M. P. Dare-Edwards, J. B. Goodenough, A. Hamnett, K. R. Seddon, R. D. Wright, *Nature* **1979**, *280*, 571–573; b) P. Falaras, *Sol. Energy Mater. Sol. Cells* **1998**, *53*, 163–175; c) K. S. Finnie, J. R. Bartlett, J. L. Woolfrey, *Langmuir* **1998**, *14*, 2744–2749.

[4] a) V. Balzani, A. Juris, M. Venturi, S. Campagna, S. Serroni, *Chem. Rev.* **1996**, *96*, 759–834; b) T. Stergiopoulos, M.-C. Bernard, A. H-Le Goff, P. Falaras, *Coord. Chem. Rev.* **2004**, *248*, 1407–1420; c) R. Argazzi, N. Y. M. Iha, H. Zabri, F. Odobel, C. A. Bignozzi, *Coord. Chem. Rev.* **2004**, *248*, 1299–1316.

[5] a) S. M. Zakeeruddin, Md. K. Nazeeruddin, R. Humphry-Baker, M. Grätzel, V. Shklover, *Inorg. Chem.* **1998**, *37*, 5251–5259; b) K. A. Maxwell, M. Sykora, J. M. DeSimone, T. J. Meyer, *Inorg. Chem.* **2000**, *39*, 71–75; c) C. M. Kepert, A. M. Bond, G. B. Deacon, L. Spiccia, B. W. Skelton, A. H. White, *Dalton Trans.* **2004**, 1766–1774; d) L. Spiccia, G. B. Deacon, C. M. Kepert, *Coord. Chem. Rev.* **2004**, *248*, 1329–1341; e) N. Onozawa-Komatsuzaki, O. Kitao, M. Yanagida, Y. Himeda, H. Sugihara, K. Kasuga, *New J. Chem.* **2006**, *30*, 689–697; f) K.-J. Jiang, N. Masaki, J.-B. Xia, S. Noda, S. Yanagida, *Chem. Commun.* **2006**, 2460–2462.

[6] a) A. S. Polo, M. K. Itokazu, N. Y. M. Iha, *Coord. Chem. Rev.* **2004**, *248*, 1343–1361 and references cited therein; b) F. Odobel, H. Zabri, *Inorg. Chem.* **2005**, *44*, 5600–5611.

[7] M. Grätzel, *J. Photochem. Photobiol., A* **2004**, *164*, 3–14.

[8] a) P. Wang, S. M. Zakeeruddin, J. E. Moser, M. K. Nazeeruddin, T. Sekiguchi, M. Grätzel, *Nat. Mater.* **2003**, *2*, 402–407; b) P. Wang, C. Klein, R. Humphry-Baker, S. M. Zakeeruddin, M. Grätzel, *J. Am. Chem. Soc.* **2005**, *127*, 808–809.

[9] J. Faiz, A. I. Philippopoulos, A. G. Kontos, P. Falaras, Z. Pikramenou, *Adv. Funct. Mater.* **2007**, *17*, 54–58.

[10] a) Md. K. Nazeeruddin, P. Péchy, M. Grätzel, *Chem. Commun.* **1997**, 1705–1706; b) M. K. Nazeeruddin, P. Pechy, T. Renouard, S. M. Zakeeruddin, R. Humphry-Baker, P. Comte, P. Liska, L. Cevey, E. Costa, V. Shklover, L. Spiccia, G. B. Deacon, C. A. Bignozzi, M. Grätzel, *J. Am. Chem. Soc.* **2001**, *123*, 1613–1624.

[11] D. L. Jameson, K. A. Goldsby, *J. Org. Chem.* **1990**, *55*, 4992–4994.

[12] A series of Ru^{II} complexes containing this class of planar tridentate nitrogen donor ligands are known: a) D. L. Jameson, J. K. Blaho, K. T. Kruger, K. A. Goldsby, *Inorg. Chem.* **1989**, *28*, 4312–4314; b) S. J. Slattery, W. D. Bare, D. L. Jameson, K. A. Goldsby, *J. Chem. Soc. Dalton Trans.* **1999**, 1347–1352; c) N. J. Beach, G. J. Spivak, *Inorg. Chim. Acta* **2003**, *343*, 244; d) M. A. Halcrow, *Coord. Chem. Rev.* **2005**, *249*, 2880–2908.

[13] a) K. Chryssou, T. Stergiopoulos, P. Falaras, *Polyhedron* **2002**, *21*, 2773–2781; b) K. Chryssou, V. J. Catalano, R. Kurtaran, P. Falaras, *Inorg. Chim. Acta* **2002**, *328*, 204–209.

[14] T. Stergiopoulos, I. M. Arabatzis, G. Katsaros, P. Falaras, *Nano Lett.* **2002**, *2*, 1259–1261.

[15] C. A. Bessel, R. F. See, D. L. Jameson, M. R. Churchill, K. J. Takeuchi, *J. Chem. Soc., Dalton Trans.* **1993**, 1563–1576. This complex was prepared by a slight modification of the published procedure and was characterized by IR spectroscopy and elemental analysis before use in the next step.

[16] O. Kohle, S. Ruile, M. Grätzel, *Inorg. Chem.* **1996**, *35*, 4779–4787.

[17] Similarly the addition of an excess of aqueous HCl (2 M) to **3** and **4** yields the desired products [Ru(bpp)(dcbpyH$_2$)(NCS)]Cl and [Ru(bpp)(dcbpyH$_2$)(CN)]Cl, respectively, together with other unidentified species, as evidenced by IR and ^{1}H NMR spectroscopy. Work is in progress to elucidate the experimental conditions in order to avoid the formation of the side products.

[18] In the case of the previously reported [Ru(bdmpp)(NCS)(dcbpyH$_2$)](PF$_6$) complex, the ν_{as}(NCS) band in the IR spectrum is not so strong. It appears as a shoulder indicating probably that the NCS ligand is coordinated via the sulfur atom as well. Preliminary photo-electrochemical experiments with the crystallized sample containing only the N-isomer showed an improved power conversion efficiency of η = 1.86% (instead of 1.70%).

[19] C. Klein, Md. K. Nazeeruddin, D. Di Censo, P. Liska, M. Grätzel, *Inorg. Chem.* **2004**, *43*, 4216–4226.

[20] a) M. Yanagida, L. P. Singh, K. Sayama, K. Hara, R. Katoh, A. Islam, H. Sugihara, H. Arakawa, M. K. Nazeeruddin, M. Grätzel, *J. Chem. Soc. Dalton Trans.* **2000**, 2817–2822; b) T. Renouard, R.-A. Fallahpour, Md. K. Nazeeruddin, R. Humprey-Baker, S. I. Gorelsky, A. B. P. Lever, M. Grätzel, *Inorg. Chem.* **2002**, *41*, 367–378.

[21] Md. K. Nazeeruddin, E. Müller, R. Humphry-Baker, N. Vlachopoulos, M. Grätzel, *J. Chem. Soc. Dalton Trans.* **1997**, 4571–4578.

[22] Md. K. Nazeeruddin, R. Humphry-Baker, P. Liska, M. Grätzel, *J. Phys. Chem. B* **2003**, *107*, 8981–8987.

[23] A. Fillinger, B. A. Parkinson, *J. Electrochem. Soc.* **1999**, *146*, 4559–4564.

[24] R. Argazzi, C. A. Bignozzi, T. A. Heimer, F. N. Castellano, G. J. Meyer, *Inorg. Chem.* **1994**, *33*, 5741–5749.

[25] B.-W. Jing, W.-Q. Wang, M.-H. Zhang, T. Shen, *Dyes Pigm.* **1998**, *37*, 177–186.

[26] G. Wolfbauer, A. M. Bond, D. R. MacFarlane, *Inorg. Chem.* **1999**, *38*, 3836–3846.

[27] R. Argazzi, G. Larramona, C. Contado, C. A. Bignozzi, *J. Photochem. Photobiol., A* **2004**, *164*, 15–21.

[28] I. M. Bell, R. J. H. Clark, D. G. Humphrey, *J. Chem. Soc. Dalton Trans.* **1999**, 1307–1310.

[29] J. D. Birchall, T. D. O'Donoghue, J. R. Wood, *Inorg. Chim. Acta* **1979**, *37*, L461–L463.

[30] T. J. Meyer, *Pure Appl. Chem.* **1986**, *58*, 1193–1206.

[31] A. Juris, V. Balzani, F. Barigelletti, S. Campagna, P. Belser, A. von Zelewsky, *Coord. Chem. Rev.* **1988**, *84*, 85–277.

[32] Md. K. Nazeeruddin, S. M. Zakeeruddin, J.-J. Lagref, P. Liska, P. Compte, C. Barolo, G. Viscardi, K. Schenk, M. Graetzel, *Coord. Chem. Rev.* **2004**, *248*, 1317–1328.

[33] S. A. Willison, H. Jude, R. M. Antonelli, J. M. Rennekamp, N. A. Eckert, J. A. Krause Bauer, W. B. Connick, *Inorg. Chem.* **2004**, *43*, 2548–2555.
[34] a) C. R. Hecker, P. E. Fanwick, D. R. McMillin, *Inorg. Chem.* **1991**, *30*, 659–666; b) S. C. Rasmussen, S. E. Ronco, D. A. Mlsna, M. A. Billadeau, W. T. Pennington, J. W. Kolis, J. D. Petersen, *Inorg. Chem.* **1995**, *34*, 821–829.
[35] a) C. R. Hecker, P. E. Fanwick, D. R. McMillin, *Inorg. Chem.* **1991**, *30*, 659–666; b) S. C. Rasmussen, S. E. Ronco, D. A. Mlsna, M. A. Billadeau, W. T. Pennington, J. W. Kolis, J. D. Petersen, *Inorg. Chem.* **1995**, *34*, 821–829.
[36] R. Argazzi, C. A. Bignozzi, T. A. Heimer, F. N. Castellano, G. J. Meyer, *Inorg. Chem.* **1994**, *33*, 5741–5749.
[37] V. J. Catalano, R. Kurtaran, R. Heck, A. Öhman, M. G. Hill, *Inorg. Chim. Acta* **1999**, *286*, 181–188.
[38] V. Shklover, Yu. E. Ovchinnikov, L. S. Braginsky, S. M. Zakeeruddin, M. Grätzel, *Chem. Mater.* **1998**, *10*, 2533–2541.
[39] M. Weidemann, H. Hückstädt, H. Homborg, *Z. Anorg. Allg. Chem.* **1998**, *624*, 846–852.
[40] S. Bonnet, J.-P. Collin, N. Gruber, J.-P. Sauvage, E. R. Schofield, *Dalton Trans.* **2003**, 4654–4662.
[41] E. Chatzivassiloglou, Ph. D. Thesis, NTUA, **2007**, Athens, Greece.
[42] M. Yanagida, T. Yamaguchi, M. Kurashige, K. Hara, R. Katoh, H. Sugihara, H. Arakawa, *Inorg. Chem.* **2003**, *42*, 7921–7931.
[43] T. A. Heimer, C. A. Bignozzi, G. J. Meyer, *J. Phys. Chem.* **1993**, *97*, 11987–11994.
[44] G. J. Meyer, *Inorg. Chem.* **2005**, *44*, 6852–6864.
[45] K. Hara, H. Sugihara, L. P. Singh, A. Islam, R. Katoh, M. Yanagida, K. Sayama, S. Murata, H. Arakawa, *J. Photochem. Photobiol., A* **2001**, *145*, 117–122.
[46] F. Ehrenberger in *Quantitative Organische Elementaranalyse*, Wiley-VCH, Weinheim, **1991**.
[47] G. M. Sheldrick, *SHELXS-86: Structure Solving Program*, University of Göttingen, Germany, **1986**.
[48] G. M. Sheldrick, *SHELXL-97: Crystal Structure Refinement Program*, University of Göttingen, Germany, **1997**.
[49] I. M. Arabatzis, T. Stergiopoulos, M. C. Bernard, D. Labou, S. G. Neofytides, P. Falaras, *Appl. Catal., B* **2003**, *42*, 187–201.
[50] a) T. Stergiopoulos, I. M. Arabatzis, H. Cachet, P. Falaras, *J. Photochem. Photobiol., A* **2003**, *155*, 163–170; b) T. Stergiopoulos, S. Karakostas, P. Falaras, *J. Photochem. Photobiol., A* **2004**, *163*, 331–340 and ref.[15] therein.

Received: March 14, 2007
Final Revision Received: October 5, 2007
Published Online: November 20, 2007

